

Drell-Yan cross-sections with fiducial cuts - impact of linear power corrections and q_T -resummation in PDF determinations

Simone Amoroso, Ludovica Aperio Bella, Maarten Boonekamp,
Stefano Camarda, Alexander Glazov, Alessandro Guida,
Renat Sadykov, Yulia Yermolchyk

Abstract

Hadron colliders measurements of neutral- and charged-current Drell-Yan production provide essential constraints in the determination of parton distribution functions. Experimentally, they have now reached percent level precision, challenging the accuracy of the theoretical predictions. In this work we benchmark the novel implementation in DYTURBO of linear fiducial power corrections in the q_T -subtraction formalism at NLO and NNLO in QCD. We illustrate how the inclusion of linear fiducial power corrections impacts predictions for precise W and Z measurements from the LHC and affect their description by modern global PDF determinations. The inclusion of q_T -resummation corrections in the theoretical predictions leads to a further improvements in the description of the lepton p_T distribution and we study how this changes the description of the data.

Presented at DIS2022: XXIX International Workshop on Deep-Inelastic Scattering and Related Subjects, Santiago de Compostela, Spain, May 2-6 2022.

1 Introduction

The Drell-Yan (DY) process consists of massive lepton pair production, through the creation of a vector boson, either γ^*/Z or W^\pm , in hadron-hadron high energy collisions. Measurements of this process help to probe the parton distribution functions (PDF) giving insight on the u - and d - valence quarks PDFs and the sea/light-quark decomposition.

The level of accuracy reached by the experiments in DY measurements needs to be matched by high precision in the theoretical predictions. The fully differential cross section considering leptonic decay is known up to NNLO in QCD [1–3] and at NLO EW [4–6]. More recently the N3LO QCD calculations have also been performed [7–10]. It has been noticed anyway that the results from different NNLO codes [11] differ between each other by an amount that can reach the percent level, much higher than the expected numerical differences. The disagreement is understood to be related to the presence of fiducial cuts applied to the final state leptons and the different subtraction schemes adopted in the calculations [12, 13]. Some cut configurations lead to a linear q_T dependence of the cross section and hence induce a bias in non-local subtraction calculations [14–17]. The q_T dependent term is referred to as *fiducial power correction* (FPC). As a solution to this problem, it has been shown that including a q_T recoil prescription, the nominal accuracy of non-local subtraction codes is recovered [12, 18, 19]. The fixed order results, regardless of the subtraction scheme used, present anyway some instabilities due to the sensitivity to enhanced q_T logarithms at small q_T [20]. In order to obtain a physical result, these logarithms need to be resummed at each perturbative order [21–24].

In this proceeding the effects of fiducial cuts and q_T resummation on DY q_T -inclusive cross section calculations are explored. As a benchmark scenario, we consider the ATLAS W and Z cross section measurement at 7 TeV [25]. These experimental data are very precise and offer important constraints on the PDF determination. The predictions are evaluated with DYTurbo [14] a versatile program for fast DY calculations. The code implements a non-local q_T subtraction method and easily allows the user to include the q_T recoil prescription [18], or the resummation effects [26]. The calculations are combined with NLO electroweak corrections computed with the ReneSANCe code.

The document is organized as follows: in section 2 the simulation setup for the predictions is described, next, in section 3, the results are presented with a particular focus on the effects related to the FPC. In section 4 a quantitative comparison with the ATLAS data is carried out. The data and the predictions are then used in section 5 for a PDF profiling study. Finally, in section 6, conclusions and further developments are discussed.

2 Simulation setup

Predictions are calculated with DYTurbo using the G_μ electroweak scheme: G_F , m_W , m_Z are the input values. The Standard Model input parameters are set to the following values

$$\begin{aligned} G_F &= 1.1663787 \times 10^{-5} \text{ GeV}^{-2}, & m_Z &= 91.1876 \text{ GeV}, \\ m_W &= 80.385 \text{ GeV}, & \Gamma_Z &= 2.4950 \text{ GeV}, \\ \Gamma_W &= 2.091 \text{ GeV}. \end{aligned} \tag{1}$$

The input PDFs are taken from the NNPDF31_nnlo_as.0118 set [27]. The values of the renormalization and factorization scale μ_R and μ_F are set equal to the dilepton invariant mass, $\mu_R = \mu_F = m_{\ell\ell}$.

The value of the q_T -slicing cut-off is set to $(q_T/m_{\ell\ell})_{\text{cut}} = 0.008$. Additional parameters to include the resummation effects need to be set. The resummation scale, μ_{Res} , is set equal to the dilepton invariant mass. Non-perturbative QCD effects at low q_T are included through a Gaussian form factor in the space of the impact parameter b , $G^{\text{NP}}(b) = \exp(-g_1 b^2)$, with $g_1 = 0.8$. NLO electroweak corrections are calculated with the ReneSANCe program and using the same EW parameters listed above as input. These include virtual weak corrections, QED initial-state radiation and initial-final interference.

The ATLAS measurement implements symmetric cuts on the final state lepton transverse momentum, $p_{T,\ell/\nu} > 25 \text{ GeV}$. The Z cross section is measured differentially in the dilepton rapidity $|y_{\ell\ell}|$ in two channels: a central channel with leptons at central pseudorapidity, $|\eta_\ell| < 2.5$, and a forward channel in which one of the two leptons is produced at high pseudorapidity, $2.5 < |\eta_\ell| < 4.9$. Three different mass bins around the Z resonance peak are considered: $m_{\ell\ell} = [46, 66, 116, 140] \text{ GeV}$. The W^\pm production cross section is measured as a function of the lepton pseudorapidity $|\eta_\ell|$. These cut configurations induce, at least in some part of phase space, linear- q_T fiducial power corrections.

The predictions are produced with high statistical accuracy; the relative statistical uncertainty is at the level of fractions of permille, completely negligible with respect to the data uncertainties and the size of the effects considered in this work.

3 NNLO results

Three different sets of predictions at NNLO are produced: the nominal fixed order using the q_T subtraction method, the fixed order including the q_T recoil prescription (equivalent to a local subtraction result) and the q_T resummed result (at a formal accuracy of NNLO+NNLL). The different calculations are shown in the example of the Z -peak bin, for the central and forward channels, in Figure 1. In the central channel a shape

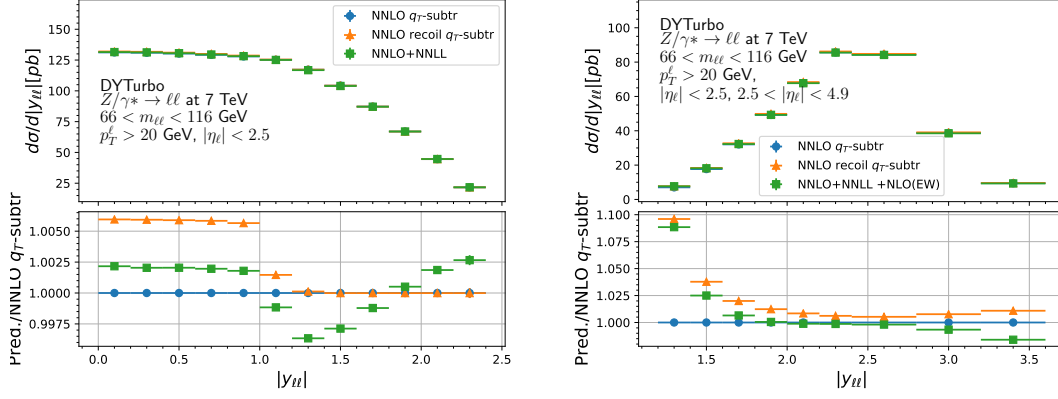


Figure 1: Z boson production cross section at NNLO (with and without implementing a q_T recoil prescription) and NNLO+NNLL. Both the central channel (left) and the forward rapidity channel (right) are reported. Some significant differences between the predictions are observed in both cases.

difference, between the three calculations, of 0.5% is observed. In the forward channel the difference between the fixed order and the resummed prediction is more striking and gets as big as 10% in the first rapidity bin. The difference between the q_T recoil calculation and the resummed one is smaller, but still of the level of few percents.

4 Data-predictions comparison

A quantitative comparison of the predictions with the experimental data is carried out using the *xFitter* framework [28]. The following χ^2 definition is used:

$$\begin{aligned}
 \chi^2(\mathbf{b}_{\text{exp}}, \mathbf{b}_{\text{th}}) = & \sum_{i=1}^{N_{\text{data}}} \frac{\left[\sigma_i^{\text{exp}} - \sigma_i^{\text{th}} (1 - \sum_k \gamma_{ik}^{\text{th}} b_{k,\text{th}} - \sum_j \gamma_{ij}^{\text{exp}} b_{j,\text{exp}}) \right]^2}{\delta_{i,\text{uncor}}^2 + \delta_{i,\text{stat}}^2} \\
 & + \sum_i \log \frac{\delta_{i,\text{uncor}}^2 (\sigma_i^{\text{th}})^2 + \delta_{i,\text{stat}}^2 \sigma_i^{\text{exp}} \sigma_i^{\text{th}}}{\delta_{i,\text{uncor}}^2 (\sigma_i^{\text{exp}})^2 + \delta_{i,\text{stat}}^2 (\sigma_i^{\text{exp}})^2} \\
 & + \sum_{j=1}^{N_{\text{exp.sys}}} b_{j,\text{exp}}^2 + \sum_{k=1}^{N_{\text{th.sys}}} b_{k,\text{th}}^2.
 \end{aligned} \tag{2}$$

Both the experimental uncertainties and theoretical uncertainties arising from PDF variation are considered. The correlated uncertainty components are accounted with two sets of nuisance parameters, \mathbf{b}_{exp} and \mathbf{b}_{th} . The impact of the correlated uncertainty sources on the theory point σ_i^{th} is described by the matrices $\gamma_{ij}^{\text{exp/th}}$. σ_i^{exp} are the data points and $\delta_{i,\text{stat}}$, $\delta_{i,\text{uncor}}$ are the statistical and uncorrelated systematic uncertainties.

The χ^2 , at its minimum, provides a test of the compatibility between the data and the predictions. The penalty term for determining the nuisance parameters is given by the last line in equation 2, this is referred to as *correlated* χ^2 component. The first line in the definition is instead quoted in the results as the data set χ^2 component. Finally, the second line, the *log penalty* term, is a small bias correction term.

Predictions for different PDFs are obtained using APPLgrids [29] generated at NLO QCD with the MCFM parton level generator [15, 30, 31]. The NNLO QCD accuracy is obtained through NNLO k -factors (kF) calculated using the DYTurbo predictions described in section 2. The kF are combined multiplicatively with NLO EW kF calculated with the ReneSANCE program.

Dataset	CT14nnlo 68%CL		
	NNLO	NNLO	NNLO+
	q_T -subtr.	recoil q_T -subtr.	NNLL
ATLAS W^+ lepton rapidity	9.4/11	8.8/11	8.8/11
ATLAS W^- lepton rapidity	8.2/11	8.7/11	8.2/11
ATLAS low mass Z rapidity	11/6	7.2/6	7.5/6
ATLAS peak CC Z rapidity	15/12	10/12	7.7/12
ATLAS peak CF Z rapidity	9.6/9	5.3/9	6.4/9
ATLAS high mass CC Z rapidity	6.0/6	6.5/6	5.8/6
ATLAS high mass CF Z rapidity	5.2/6	5.6/6	5.3/6
Correlated χ^2	39	40	32
Log penalty χ^2	-4.33	-3.39	-4.20
Total χ^2/dof	99/61	88/61	77/61
χ^2 p-value	0.00	0.01	0.08

Table 1: Results of the data-predictions comparison. The CT14nnlo 68%CL PDF is used. An improvement in the χ^2 agreement is observed when including resummation effects in the predictions.

PDF set	Total χ^2 (ndf=61)		
	NNLO q_T subtr.	NNLO recoil q_T -subtr	NNLO+NNL
CT10nnlo68%CL	100	85	76
CT14nnlo68%CL	99	88	77
CT18NNLO68%CL	102	90	79
MMHT14nnlo68%CL	124	99	94
NNPDF30nnlo	139	133	111
ABMP16_5_NNLO	124	106	92
HERAII PDF	199	201	160
CT18ANNLO68	96	84	74
MSHT20nnlo	111	87	79
NNPDF31	91	84	71
NNPDF40nnlo	89	83	69

Table 2: Total χ^2 for the comparison between the predictions and the ATLAS data, using different PDF sets. The three different theory definitions are tested. The resummed prediction always gives the best agreement with the data. The first half of the table considers PDFs that did not include ATLAS 7 TeV W and Z data, while in the second half are PDFs that used these data in their determination.

As a first test, the CT14nnlo PDF set [32] is used in the comparison. The χ^2 results are reported in Table 1.

The three sets of predictions introduced in section 3 are used for the study. A reduction of ~ 10 points in the total χ^2 when using a theory that include a q_T recoil prescription is observed. A further improvement of other ~ 10 points is obtained when considering the q_T resummation effects. The trend of the results is in line with the theoretical expectation of section 1. The study is extended testing other PDF sets. The total χ^2 are reported in Table 2. In all the cases a similar reduction of the total χ^2 , of about 20 – 30 when including the q_T -resummation, is observed.

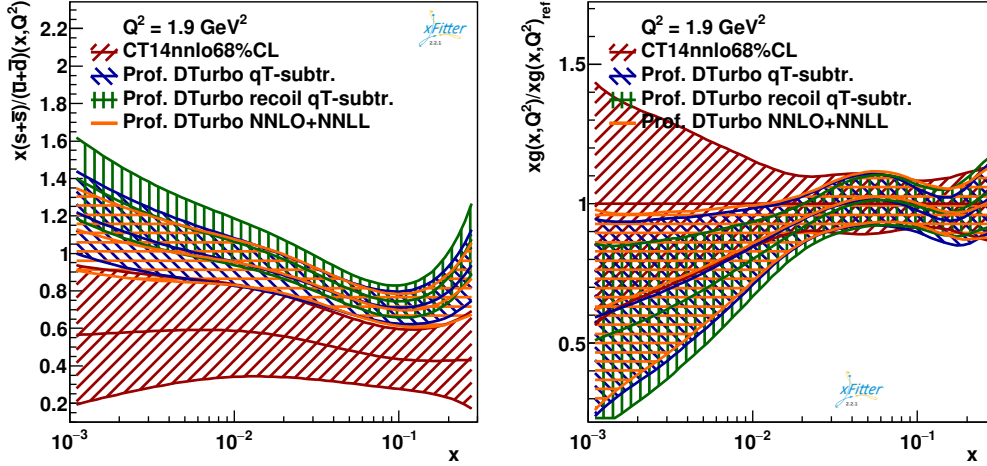


Figure 2: R_s (left) and the gluon PDF ratio to the CT14 set (right). The CT14 PDF set and the profiled PDF using the ATLAS data and different NNLO definitions are shown.

5 PDF profiling

The value of the nuisance parameters, \mathbf{b}_{th} , at the χ^2 minimum, equation 2, are used to obtain an optimized version of the central PDF f'_0

$$f'_0 = f_0 + \sum_k b_{k,th}^{min} \left(\frac{f_k^+ - f_k^-}{2} - b_{k,th}^{min} \frac{f_k^+ + f_k^- - 2f_0}{2} \right). \quad (3)$$

Here f_0 is the original central PDF and f_k^\pm are the eigenvector up/down variation sets. Furthermore the updated PDFs have reduced uncertainties. The profiling procedure is used to test the impact of new data set on existing PDF sets.

Here the CT14nnlo 68% CL PDF set is used for the profiling; this set does not include the ATLAS W and Z 7 TeV data. The different NNLO(+NNLL) predictions introduced in section 3 are used and the differences in the outcome of the profiling are examined. In Figure 2 the profiling results for two relevant quantities that are constrained by DY data, are shown: the ratio $R_s = x(s + \bar{s})/(\bar{u} + \bar{d})$ and the gluon PDF. The big impact of these data sets, in particular on the R_s value, is clearly visible. A difference between the profiled PDFs when using the different NNLO calculations is also noticeable. A general observation is that the profiled PDFs using the resummed theory are somewhat closer to the one using the fixed order q_T subtraction theory.

6 Conclusion

In this work the effects of fiducial cuts in the calculations for DY cross section has been investigated. Predictions for the ATLAS W and Z 7 TeV cross section have been produced with DYTurbo. A quantitative comparison with data, including PDF uncertainties, shows a better agreement when the q_T resummation effects are taken into account in the predictions. The profiling procedure has been carried out to estimate the impact of using different theory definitions in the PDF determination. This exercise shows small, but still noticeable differences. As further steps, the effect of fiducial cuts on other measurement phase spaces can be investigated, and the impact on the PDF determination can be evaluated through a PDF fit to DY data.

References

- [1] Melnikov, K. et al. *Physical Review Letters* **2006**, *96*, DOI: 10.1103/physrevlett.96.231803.
- [2] Melnikov, K. et al. *Physical Review D* **2006**, *74*, DOI: 10.1103/physrevd.74.114017.
- [3] Catani, S. et al. *Physical Review Letters* **2009**, *103*, DOI: 10.1103/physrevlett.103.082001.
- [4] Dittmaier, S. et al. *Physical Review D* **2002**, *65*, DOI: 10.1103/physrevd.65.073007.
- [5] Baur, U. et al. *Physical Review D* **2004**, *70*, DOI: 10.1103/physrevd.70.073015.
- [6] Zykunov, V. A. *Phys. Atom. Nucl.* **2006**, *69*, 1522.
- [7] Duhr, C. et al. *Journal of High Energy Physics* **2020**, *2020*, DOI: 10.1007/jhep11(2020)143.
- [8] Chen, X. et al. *Physical Review Letters* **2022**, *128*, DOI: 10.1103/physrevlett.128.052001.
- [9] Duhr, C. et al. *Journal of High Energy Physics* **2022**, *2022*, DOI: 10.1007/jhep03(2022)116.
- [10] Chen, X. et al. *Physical Review Letters* **2022**, *128*, DOI: 10.1103/physrevlett.128.252001.
- [11] Alekhin, S. et al. *The European Physical Journal C* **2021**, *81*, DOI: 10.1140/epjc/s10052-021-09361-9.
- [12] Ebert, M. A. et al. *Journal of High Energy Physics* **2021**, *2021*, DOI: 10.1007/jhep04(2021)102.
- [13] Billis, G. et al. *Physical Review Letters* **2021**, *127*, DOI: 10.1103/physrevlett.127.072001.
- [14] Camarda, S. et al. *The European Physical Journal C* **2020**, *80*, DOI: 10.1140/epjc/s10052-020-7757-5.
- [15] Campbell, J. M. et al. *Physical Review D* **1999**, *60*, DOI: 10.1103/physrevd.60.113006.
- [16] Grazzini, M. et al. *The European Physical Journal C* **2018**, *78*, DOI: 10.1140/epjc/s10052-018-5771-7.
- [17] Catani, S. et al. *Journal of High Energy Physics* **2015**, *2015*, 1–47.
- [18] Camarda, S. et al. **2021**.
- [19] Buonocore, L. et al. Linear power corrections for two-body kinematics in the q_T subtraction formalism, 2021.
- [20] Salam, G. P. et al. *Journal of High Energy Physics* **2021**, *2021*, DOI: 10.1007/jhep11(2021)220.
- [21] Dokshitzer, Y. et al. *Physics Letters B* **1978**, *79*, 269–272.
- [22] Parisi, G. et al. *Nucl. Phys. B* **1979**, *154*, 427–440.
- [23] Collins, J. et al. *Nuclear Physics B* **1985**, *250*, 199–224.
- [24] Catani, S. et al. *Nuclear Physics B* **2014**, *881*, 414–443.
- [25] collaboration, A. *The European Physical Journal C* **2017**, *77*, DOI: 10.1140/epjc/s10052-017-4911-9.
- [26] Camarda, S. et al. *Physical Review D* **2021**, *104*, DOI: 10.1103/physrevd.104.1111503.
- [27] Ball, R. D. et al. *The European Physical Journal C* **2017**, *77*, DOI: 10.1140/epjc/s10052-017-5199-5.
- [28] Alekhin, S. et al. HERAFitter, Open Source QCD Fit Project, 2015.
- [29] Carli, T. et al. *The European Physical Journal C* **2010**, *66*, 503–524.
- [30] Campbell, J. M. et al. *Journal of High Energy Physics* **2011**, *2011*, DOI: 10.1007/jhep07(2011)018.
- [31] Campbell, J. M. et al. A Multi-Threaded Version of MCFM, 2015.

[32] Dulat, S. et al. *Physical Review D* **2016**, *93*, DOI: 10.1103/physrevd.93.033006.